Symmetry of superconducting states with two orbitals on a tetragonal lattice: Application to $LaFeAsO_{1-x}F_x$

Yi Zhou,[1,2] Wei-Qiang Chen,[1] and Fu-Chun Zhang[1]
[1]*Department of Physics, Center of Theoretical and Computational Physics, The University of Hong Kong, Hong Kong, China*
[2]*Department of Physics, Chinese University of Hong Kong, Hong Kong, China*
(Received 22 June 2008; published 19 August 2008)

We use group theory to classify the superconducting states of systems with two orbitals on a tetragonal lattice. The orbital part of the superconducting gap function can be either symmetric or antisymmetric. For the orbital symmetric state, the parity is even for spin singlet and odd for spin triplet; for the orbital antisymmetric state, the parity is odd for spin singlet and even for spin triplet. The gap basis functions are obtained with the use of the group chain scheme by taking into account the spin-orbit coupling. In the weak pairing limit, the orbital antisymmetric state is only stable for the degenerate orbitals. Possible application to iron-based superconductivity is discussed.

DOI: 10.1103/PhysRevB.78.064514 PACS number(s): 74.20.Rp

I. INTRODUCTION

Symmetry plays an important role in the study of superconductivity. By using the symmetry of the superconducting (SC) gap function, Ginzburg-Landau theory can be constructed and electromagnetic response and topological excitations can be inspected. In the past decades, the symmetry analyses to classify unconventional SC states have been focused on single-band superconductors and have shed much light on our understanding of heavy-fermion and ruthenate superconductors.[1]

Very recently, a new class of iron-based high-temperature superconductors has been discovered with T_c as high as above 50 K.[2–9] Experimentally, spin-density wave (SDW) order has been observed in the parent compound LaFeAsO but vanishes upon fluorine doping where the superconductivity appears.[10,11] Specific heat measurement as well as nuclear magnetic resonance suggested line nodes of the SC gap.[12–15] The transition temperature estimated based on the electron-phonon coupling is low and unlikely to explain the observed superconductivity.[16] It has been proposed that the superconductivity is of magnetic origin and is unconventional. Local density approximation (LDA) shows that iron's $3d$ electrons dominate the density of states near the Fermi surfaces in the parent compound LaFeAsO.[17–22] In their calculations, there are three holelike Fermi surfaces centered at the Γ point and two electronlike Fermi surfaces around the M point. By F doping, the area of the three holelike Fermi surfaces shrinks while the area of the two electronlike Fermi surfaces expands. The band structure obtained from the LDA may be well modeled by a tight-binding model with two or three orbitals (d_{xz}, d_{yz}, and d_{xy}).[23–30] Because of the multiple orbitals in the low-energy physics, it is natural to raise the question how to generalize the symmetry consideration from single-band to multiband cases.

In this paper, we will generalize the symmetry analyses developed for the single-band SC state to systems with two orbitals. We will use group theory to classify the allowed symmetry of the gap functions of the two-orbital SC state on a tetragonal lattice by including a spin-orbit coupling between the paired electrons. While our focus will be on the Fe-based compounds, some of our analyses may be applied to more general systems with two orbitals.

We arrange this paper as the follows. In Sec. II, we discuss the symmetries governing the system and how these symmetries affect the Hamiltonian and gap functions. In Sec. III, we consider the possible two-orbital SC states on a tetragonal lattice. Section IV is devoted to summary and discussions. We also supply some appendixes for details. In Appendix A, we show how the symmetries give rise to the requirements to the noninteracting Hamiltonian. In Appendix B, we specify the point group D_{4h} of lattice according to space group $P4/nmm$. In Appendix C, we discuss how the gap functions transfer under symmetry operations. In Appendix D, we discuss the energy-gap functions in the degenerate bands.

II. SYMMETRY OF GAP FUNCTION $\Delta(k)$

We consider a tetragonal lattice, appropriate for doped LaFeAsO. Since our primary interest is in the SC state, we will not consider the translational symmetry broken state such as the spin-density wave state observed in the parent compound of LaFeAsO. The system is invariant under both time reversal and space inversion. The inversion symmetry suggests that the SC pairing is either even or odd in parity. We shall assume in this paper that the time-reversal symmetry remains unbroken.

We consider a system described by Hamiltonian

$$H = H_0 + H_{\text{pair}} + H_{\text{so}}, \tag{1}$$

where H_0 is noninteracting part, H_{pair} is a pairing Hamiltonian, and H_{so} is the spin-orbit coupling of the Cooper pairs. We shall consider the SC state preserves all the symmetries in H_0 except the U(1) symmetry in electric charge and the spin rotational symmetry due to a weak H_{so}. We assume H_0 to be given by a tight-binding Hamiltonian

$$H_0 = \sum_{\mathbf{k}\alpha_1\alpha_2 s} c^{\dagger}_{\mathbf{k}\alpha_1 s}\xi_{\mathbf{k}\alpha_1\alpha_2}c_{\mathbf{k}\alpha_2 s}, \tag{2}$$

where $\alpha=1,2$ are the orbital indices, which correspond to the two orbitals $3d_{xz}$ and $3d_{yz}$ in Fe, $s=\uparrow,\downarrow$, are the spin indices.

Note that for LaFeAsO, the actual crystal structure has two Fe atoms in a unit cell due to the As atomic positions, which are allocated above and below the Fe-plane alternatively. For convenience, here we use the extended Brillouin zone, and the summation $\mathbf{k}$ is in the extended zone. H_0 is invariant under symmetry transformation. This requires certain symmetries on $\xi_{\mathbf{k}\alpha_1\alpha_2}$, which we will discuss in detail in Appendix A. We note that a more appropriate model should also include the d_{xy} orbital,[25] but we shall leave the symmetry analyses of the three orbitals for future study and consider a simplified version of the two-orbital case in this paper.

The gap function of the two-orbital SC state can be generally written as

$$\Delta_{s_1s_2}^{\alpha_1\alpha_2}(\mathbf{k}) = -\sum_{\substack{\mathbf{k}'\alpha_3\alpha_4\\ s_3s_4}} V_{s_2s_1s_3s_4}^{\alpha_2\alpha_1\alpha_3\alpha_4}(\mathbf{k},\mathbf{k}')\langle c_{\mathbf{k}'\alpha_3s_3}c_{-\mathbf{k}'\alpha_4s_4}\rangle, \quad (3)$$

where $V_{s_2s_1s_3s_4}^{\alpha_2\alpha_1\alpha_3\alpha_4}(\mathbf{k},\mathbf{k}')$ is the effective attractive interaction. Hereafter we will use the matrix notation $\Delta(\mathbf{k})$ for the gap function.

To classify the symmetry of the SC gap function for multiple orbitals, we recall that in the single orbital case, the spin-orbit coupling of the Cooper pair plays an important role to the non-s-wave superconductors, and the symmetry of the gap function is determined by the crystal point group of the lattice and the spin part of the gap function. In the two-orbital system, the orbital degree of freedom is usually coupled to the crystal momentum, hence to the spin via the spin-orbit coupling. Therefore, the spin, spatial, and the orbital parts are generally all related in the gap function.

Let us first discuss the crystal symmetry. The crystal structure of LaFeAsO is shown in Fig. 1. The tetragonal crystal symmetry is characterized by the point group D_{4h}. The tetragonal point group may be specified according to the space group $P4/nmm$ of the compound, and the details will be discussed in Appendix B. There are five irreducible representations of D_4 group, denoted by Γ, including four one-dimensional representations (A_1, A_2, B_1, and B_2) and one two-dimensional (2D) representation (E).[32] The tetragonal lattice symmetry requires H_0 to be a "scalar" or A_1 representation of D_4. In the absence of spin-orbit coupling, spin is rotational invariant and we have both the point-group symmetry and the spin rotational symmetry.[33]

We now discuss the orbital degrees of freedom in connection with the crystal symmetry. The two orbitals d_{xz} and d_{yz} transform as E representation of D_4. In general the orbital indices d_{xz} and d_{yz} are not good quantum numbers because of the mixed term of the two orbitals in H_0, and the two energy bands are not degenerate. In that case it is necessary to include the coupling of the orbital to spatial and spin degrees of freedom.

Without loss of generality, the gap function can be written as a linear combination of the direct products of the orbital part Ω and the spin part Δ^{spin} in a given representation Γ of the point group D_4,

$$\Delta(\Gamma;\mathbf{k}) = \sum_{m,\Gamma_{LS},\Gamma_\Omega} \eta(\Gamma,m)\langle\Gamma,m|\Gamma_{LS},m_{LS};\Gamma_\Omega,m_\Omega\rangle \times \Delta^{\text{spin}}(\Gamma_{LS},m_{LS};\mathbf{k})\otimes\Omega(\Gamma_\Omega,m_\Omega), \quad (4)$$

where both Δ^{spin} and Ω are 2×2 matrices, $\Delta_{s_1s_2}^{\text{spin}}$ dictates the pairing in spin space and $\Omega_{\alpha_1\alpha_2}$ dictates the pairing in orbital space, Γ_{LS} and Γ_Ω are irreducible representations of D_4 in spin and orbital spaces, respectively, m, m_{LS}, and m_Ω are bases of representations Γ, Γ_{LS}, and Γ_Ω, respectively. $\langle\Gamma,m|\Gamma_{LS},m_{LS};\Gamma_\Omega,m_\Omega\rangle$ is the Clebsch-Gordan (CG) coefficient. Note that the $\mathbf{k}$ dependence is contained in Δ^{spin} but not in Ω. Here $\eta(\Gamma,m)$ is the coefficient of the basis m of the representation Γ. The antisymmetric statistics of two electrons requires

$$\Delta^T(-\mathbf{k}) = -\Delta(\mathbf{k}). \quad (5)$$

Below we will first discuss $\Delta^{\text{spin}}(\Gamma_{LS};\mathbf{k})$ and $\Omega(\Gamma_\Omega)$ separately and then combine the two to form an irreducible representation Γ of D_4. We follow Sigrist and Ueda[1] and write $\Delta^{\text{spin}}(\mathbf{k})$ in terms of the basis functions $\psi(\Gamma,m;\mathbf{k})$ for the spin singlet $S=0$ and $\mathbf{d}(\Gamma,m;\mathbf{k})$ for the spin triplet $S=1$,

$$\Delta^{\text{spin}}(\Gamma,m;\mathbf{k}) = i[\sigma_0\psi(\Gamma,m;\mathbf{k}) + \sigma\cdot\mathbf{d}(\Gamma,m;\mathbf{k})]\sigma_2. \quad (6)$$

Here $\psi(\mathbf{k})$ is a scalar and $\mathbf{d}(\mathbf{k})$ is a vector under the transformation of spin rotation. For this reason, it is more convenient to use $\psi(\mathbf{k})$ and $\mathbf{d}(\mathbf{k})$ instead of $\Delta^{\text{spin}}(\mathbf{k})$ to classify the pairing states.

Due to the fermionic antisymmetric nature, the gap function must be antisymmetric under the two-particle interchange or under combined operations of space inversion, in-

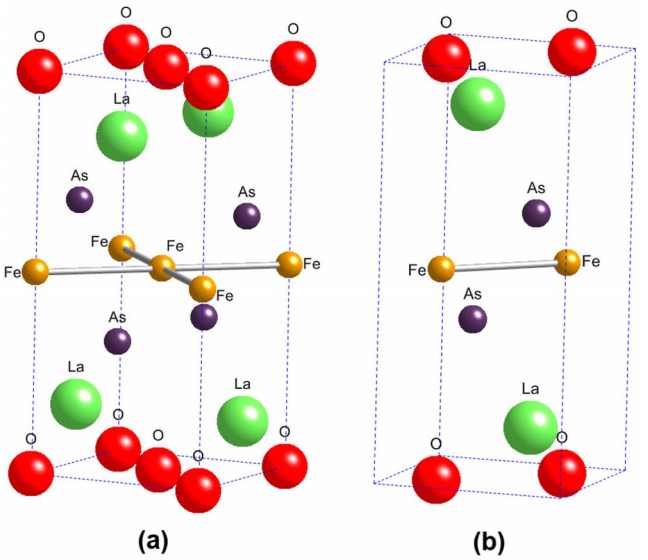

FIG. 1. (Color online) Lattice structure of LaFeAsO. It is a tetragonal lattice with two Fe atoms per unit cell. The lattice constants are $a=b\simeq4.03$ Å and $c\simeq8.74$ Å (Ref. 11), where a is the distance between two next-nearest-neighbor Fe atoms. (a) Origin choice 1 of space group $P4/nmm$ at $\bar{4}m2$ and at $(-a/4,a/4,0)$ from center $(2/m)$. It can be chosen either at an Fe or at an O atom. (b) Origin choice 2 of space group $P4/nmm$ at center $(2/m)$ and at $(a/4,-a/4,0)$ from $\bar{4}m2$. It can be chosen either at the midpoint of two nearest-neighbor Fe atoms or at the midpoint of two nearest-neighbor O atoms. Here $2/m$ denotes the twofold rotation C_2 and reflection m (see Appendix B for details). The origin choices 1 and 2 are different from each other by a shift of $(-a/4,a/4,0)$ (Ref. 31).

terchange of the spin indices, and interchange of the orbital indices of the two particles. Let $P_{1,2}$ be the two-particle interchange operator and $P_{\text{space}}, P_{\text{spin}}, P_{\text{orbital}}$ be the interchange operator acting on the space, spin, and orbital, respectively, then the fermion statistics requires

$$P_{1,2} = P_{\text{space}} P_{\text{spin}} P_{\text{orbital}} = -1. \tag{7}$$

Since the system is of inversion symmetry, the pairing states must have either even parity $P_{\text{space}}=+1$ or odd parity $P_{\text{space}}=-1$. Furthermore, the total spin S of the Cooper pair is a good number, and this is so even in the presence of H_{so}, which breaks spin rotational symmetry but keeps inversion symmetry so that it does not mix the $S=1$ with $S=0$ states. Therefore, under the two-particle interchange, the spin part of the gap function must be either symmetric ($P_{\text{spin}}=+1$ with $S=1$) or antisymmetric ($P_{\text{spin}}=-1$ with $S=0$), represented by the vector $\mathbf{d}$ or the scalar ψ in Eq. (6), respectively. Because of the inversion and spin symmetries, we have $P_{\text{orbital}}=\pm 1$.

The orbital part of the pairing matrix Ω is spanned in the vector space of (d_{xz}, d_{yz}), which is an irreducible representation E of the point group D_4. Thus Ω belongs to an irreducible representation given by $E \otimes E = A_1 \oplus A_2 \oplus B_1 \oplus B_2$, which are all one dimensional, hence simplifies the classification of the pairing states. According to the CG coefficients of D_4 group, up to a global factor, $\Omega=\sigma_0$ in representation A_1, $\Omega=\sigma_3$ in B_1, and $\Omega=\sigma_1$ in B_2, which are all orbital symmetric: $P_{\text{orbital}}=+1$. $\Omega=\sigma_2$ in A_2 representation, which is orbital antisymmetric: $P_{\text{orbital}}=-1$. In brief, A_1 and B_1 of Ω are representations for intraorbital pairing, B_2 is for symmetric interorbital pairing, and A_2 is for antisymmetric interorbital pairing. For convenience, we choose Ω to be Hermitian so that $\psi(\mathbf{k})$ and $\mathbf{d}(\mathbf{k})$ will be real. (Wan and Wang[34] pointed out that Pauli matrices transfer as four one-dimensional irreducible representations.)

The crystal point group of the lattice will dictate the allowed symmetry in $\mathbf{k}$ space. The transformation of ψ and $\mathbf{d}$ under symmetry operations can be found in Appendix C. In Sec. III, we will study the basis functions $\psi(\Gamma, m; \mathbf{k})$ and $\mathbf{d}(\Gamma, m; \mathbf{k})$ and combine them with the orbital part Ω to obtain the irreducible representations of group D_4.

III. POSSIBLE TWO-ORBITAL SC STATES ON A TETRAGONAL LATTICE

We will use the group chain scheme to study the representation and the basis function of ψ and $\mathbf{d}$ by assuming a spin-orbit coupling. In the group chain scheme, we begin with a rotational invariant system in both spin and spatial spaces. The representation of its symmetry group G can be decoupled into a spatial part $D_{(L)}$ and a spin part $D_{(S)}$, with $\mathbf{L}$ as the relative angular momentum of the Cooper pair,

$$D_{(G)} = D_{(L)} \otimes D_{(S)}. \tag{8}$$

In the presence of the spin-orbit coupling, $D_{(L)}$ and $D_{(S)}$ are no longer the irreducible representation of the rotational group, but the total angular momentum $\mathbf{J}=\mathbf{L}+\mathbf{S}$ is, and $D_{(J)}$ is the corresponding irreducible representation of the rotational group.

TABLE I. Superconducting gap basis functions $\psi(\mathbf{k})$ on tetragonal lattice for even-parity, orbital symmetric, and spin singlet pairing states. Γ is the representation of D_4. The listed notations are natural, or Schönflies and Koster (in parentheses). Ω is the orbital representation, σ_0 is the identity matrix, and $\sigma_{1,2,3}$ are the Pauli matrices. Listed gaps properties are for the two completely degenerate orbitals. k_z-dependent basis functions are marked with 3D listed for completeness.

Γ	Basis $\psi(\mathbf{k})$	Ω	Gap
0 (A_{1g}, Γ_1^+)	$1, k_x^2+k_y^2; k_z^2$ (3D)	σ_0	Line nodal or full gap
	$k_x^2-k_y^2$	σ_3	
	$k_x k_y$	σ_1	
$\tilde{0}$ (A_{2g}, Γ_2^+)	$k_x k_y (k_x^2-k_y^2)$	σ_0	Line, full
	$k_x k_y$	σ_3	
	$k_x^2-k_y^2$	σ_1	
2 (B_{1g}, Γ_3^+)	$k_x^2-k_y^2$	σ_0	Line, full
	$1, k_x^2+k_y^2; k_z^2$ (3D)	σ_3	
	$k_x k_y (k_x^2-k_y^2)$	σ_1	
$\tilde{2}$ (B_{2g}, Γ_4^+)	$k_x k_y$	σ_0	Line, full
	$k_x k_y (k_x^2-k_y^2)$	σ_3	
	$1, k_x^2+k_y^2; k_z^2$ (3D)	σ_1	
1 (E_g, Γ_5^+)	$(k_x k_z, k_y k_z)$ (3D)	$\sigma_0, \sigma_3, \sigma_1$	

We now turn on a crystal field with tetragonal lattice symmetry group D_4 so that the rotational group SO(3) is reduced to D_4, and $D_{(L)} \otimes D_{(S)}$ is reduced to a direct product of irreducible representations Γ_{LS} of group D_4,

$$D_{(L)} \otimes D_{(S)} \to \bigoplus_{\Gamma_{LS}} D_{(\Gamma_{LS})}. \tag{9}$$

Including the coupling to the orbital part Ω, the representation $D_{(\Gamma_{LS})} \otimes D_{(\Gamma_\Omega)}$ is decomposed into irreducible representations,

$$D_{(\Gamma_{LS})} \otimes D_{(\Gamma_\Omega)} = \bigoplus_{\Gamma} D_{(\Gamma)}. \tag{10}$$

$D_{(\Gamma_\Omega)}$ is one dimensional; thus these representations have a very simple form.

Let us consider the even-parity case. From Eq. (7), the SC gap function can be either orbital symmetric $P_{\text{orbital}}=+1$, spin singlet, or orbital antisymmetric $P_{\text{orbital}}=-1$, spin triplet. We list the SC gap basis functions for spin singlet and spin triplet according to the irreducible representations Γ in Tables I and II, respectively. The listed even pairing states include s wave (extended s wave), d wave, and g wave. Here 0, $\tilde{0}$, 2, $\tilde{2}$, and 1 are natural notation for the five irreducible representations of D_{4h}; A_1, A_2, B_1, B_2, and E are Schönflies notation; Γ_{1-5} are Koster notation. According to Eq. (3), the gap function of the SC state is a linear combination of the basis functions in one irreducible representation Γ, and the

TABLE II. Superconducting gap basis functions $\mathbf{d}(\mathbf{k})$ on tetragonal lattice for even-parity, orbital antisymmetric, and spin triplet pairing states. Notations are the same as in Table I.

Γ	Basis $\mathbf{d}(\mathbf{k})$	Ω	Gap
$0\ (A_{1g},\ \Gamma_1^+)$	$\hat{z},(k_x^2+k_y^2)\hat{z},(k_x^4+k_y^4)\hat{z},k_x^2k_y^2\hat{z}$	σ_2	Line, full
$\tilde{0}\ (A_{2g},\ \Gamma_2^+)$	$k_z(k_x\hat{y}-k_y\hat{x})$ (3D)	σ_2	
$2\ (B_{1g},\ \Gamma_3^+)$	$(k_x^2-k_y^2)\hat{z};k_z(k_x\hat{x}-k_y\hat{y})$ (3D)	σ_2	Line
$\tilde{2}\ (B_{2g},\ \Gamma_4^+)$	$k_xk_y\hat{z};k_z(k_x\hat{x}+k_y\hat{y})$ (3D)	σ_2	Line
$1\ (E_g,\ \Gamma_5^+)$	$(\hat{x},\hat{y}),(k_x^2\hat{x},k_x^2\hat{y}),(k_y^2\hat{x},k_y^2\hat{y}),$ $(k_xk_y\hat{x},k_xk_y\hat{y});(k_z^2\hat{x},k_z^2\hat{y}),$ $(k_xk_z\hat{z},k_yk_z\hat{z})$ (3D)	σ_2	Line, full

basis functions belonging to different representations in Γ, e.g., A_{1g} and B_{2g}, will not mix with each other.

We are particularly interested in 2D or quasi-2D limiting cases, relevant to Fe-based SC compounds, where the gap function is k_z independent, and the Fermi surface is cylinderlike. However, for completeness we also list in Tables I and II those three-dimensional basic functions marked with 3D. In the last column of each table, we list the allowed energy zeroes in the quasiparticle dispersion determined by the gap functions for the special case that the two energy bands are completely degenerate. The detailed calculations for the quasiparticle energies in the degenerate cases are given in Appendix D. We will discuss the quasiparticle properties for the nondegenerate cases in the discussion section below.

Similarly, for the odd-parity pairing $P_{\text{space}}=-1$, we can have either orbital antisymmetric $P_{\text{orbital}}=-1$, spin singlet, or orbital symmetric $P_{\text{orbital}}=1$, spin triplet, which are listed in Tables III and IV, respectively. For the spin triplet, we list p-wave, f-wave, and h-wave states.

IV. SUMMARY AND DISCUSSIONS

In summary, we have studied the pairing symmetry of the two-orbital superconducting states on a tetragonal lattice. Based on the symmetry consideration, we have classified symmetry allowed pairing states with the space inversion, spin, orbital, and the lattice symmetries by including a spin-orbit coupling. In addition to the even parity for the spin singlet and odd parity for the spin triplet pairings, familiar in the single-band superconducting gap functions, which corresponds to orbital symmetric pairing in the two-orbital systems, there are also even parity for spin triplet and odd parity for the spin singlet pairings, corresponding to orbital antisymmetric pairing. The symmetry allowed gap basis functions are listed in Tables I–IV in the text. In the orbital symmetric states, the gap basis functions within the same representation of the point group but with different orbital representations are allowed to combine to form a gap function.

TABLE III. Superconducting gap basis functions $\psi(\mathbf{k})$ on tetragonal lattice for odd-parity, orbital antisymmetric, and spin singlet pairing state. Notations are the same as in Table I.

Γ	Basis $\psi(\mathbf{k})$	Ω	Gap
$0\ (A_{1u},\ \Gamma_1^-)$	k_z (3D)	σ_2	
$\tilde{0}\ (A_{2u},\ \Gamma_2^-)$	$k_z(k_x^4-6k_x^2k_y^2+k_y^4)$ (3D)	σ_2	
$2\ (B_{1u},\ \Gamma_3^-)$	$k_z(k_x^2-k_y^2)$ (3D)	σ_2	
$\tilde{2}\ (B_{2u},\ \Gamma_4^-)$	$k_xk_yk_z$ (3D)	σ_2	
$1\ (E_u,\ \Gamma_5^-)$	(k_x,k_y)	σ_2	Line

TABLE IV. Superconducting gap basis functions $\mathbf{d}(\mathbf{k})$ on tetragonal lattice for odd-parity, orbital symmetric, and spin triplet pairing states.

Γ	Basis $\mathbf{d}(\mathbf{k})$	Ω	Gap
	$k_x\hat{x}+k_y\hat{y};k_z\hat{z}$ (3D)	σ_0	
$0\ (A_{1u},\ \Gamma_1^-)$	$k_x\hat{x}-k_y\hat{y}$	σ_3	Line, full
	$k_y\hat{x}+k_x\hat{y}$	σ_1	
	$k_y\hat{x}-k_x\hat{y}$	σ_0	
$\tilde{0}\ (A_{2u},\ \Gamma_2^-)$	$k_y\hat{x}+k_x\hat{y}$	σ_3	Line, full
	$k_x\hat{x}-k_y\hat{y}$	σ_1	
	$k_x\hat{x}-k_y\hat{y}$	σ_0	
$2\ (B_{1u},\ \Gamma_3^-)$	$k_x\hat{x}+k_y\hat{y};k_z\hat{z}$ (3D)	σ_3	Line, full
	$k_y\hat{x}-k_x\hat{y}$	σ_1	
	$k_y\hat{x}+k_x\hat{y}$	σ_0	
$\tilde{2}\ (B_{2u},\ \Gamma_4^-)$	$k_y\hat{x}-k_x\hat{y}$	σ_3	Line, full
	$k_x\hat{x}+k_y\hat{y};k_z\hat{z}$ (3D)	σ_1	
$1\ (E_u,\ \Gamma_5^-)$	$(k_x\hat{z},k_y\hat{z});(k_z\hat{x},k_z\hat{y})$ (3D)	$\sigma_0,\sigma_3,\sigma_1$	Line

Below we shall discuss some limiting cases. First, we consider the weak pairing coupling limit. In this case, we can diagonalize H_0 first to obtain the two energy bands. H_{pair} in Eq. (1) is to induce a pairing of electrons near the Fermi surfaces within a very small energy window. If the two energy bands are not degenerate, then the two Fermi surfaces do not coincide with each other, and the pairing will only occur between electrons in the same band since the energy mismatch of the two electrons with opposite momentum in the two bands will not lead to the SC instability in the weak-coupling limit. The issue is then reduced to the two decoupled single-band problem. Because the intraband pairing is between symmetric orbitals, all the states with orbital antisymmetric pairings such as those listed in Tables II and III will not be realized. There is a one-to-one correspondence between the present work and the single-band analysis.[1] In terms of the orbital picture, the intraband pairing gap function is described by a linear combination of the orbital representations $\sigma_0,\sigma_1,\sigma_3$ in each representation of Γ.

The strong pairing coupling case is more complicated and possibly more interesting. The symmetry analyses we outlined in this paper may serve as a starting point. The pairing interaction may overcome the energy mismatch of the paired interband electrons to lead to the superconductivity. In a re-

cent exact diagonalization calculation for a two-orbital Hubbard model on a small size system, Daghofer *et al.*[35] found an interorbital pairing with spin triplet and even parity with the gap function to be $\cos k_x + \cos k_y$. Their pairing state corresponds to E_g representation in Table II and provides a concrete example of the orbital antisymmetric pairing state. Generally we may argue that the gap structure will be gapless with Fermi pockets for 2D systems unless the pairing coupling is strong enough to overcome all the mismatched paired electrons in the momentum space. An example was given by Dai *et al.*[23] and also discussed by Wan *et al.*[34] This seems to essentially rule out any possibility for line nodes in the orbital antisymmetric pairing state in the strong pairing coupling limit. A nodal in quasiparticle energy requires the gap function to vanish. As a result, the pairing strength near this nodal will not be strong enough to overcome the energy mismatch of the interband paired electrons. Therefore, a nodal in quasiparticle energy implies a Fermi pocket in this case.

Another interesting limit is the two orbitals are completely degenerate: $\xi_{\mathbf{k}\alpha_1,\alpha_2} = \xi_{\mathbf{k}} \delta_{\alpha_1,\alpha_2}$. The system has an orbital SU(2) symmetry. In this case, our analyses are most relevant, and all the classified states listed in Tables I–IV could be stable even in the weak pairing interaction. Because of the orientational dependence of the orbitals in crystal, such degeneracies may not be easy to realize. A possible realization is on the materials with twofold pseudospin symmetry or two-valley degeneracy such as in graphene. While the point group will depend on the precise crystal symmetry concerned, some general features discussed in this paper may be applied to those systems.

We now discuss the band structure in the extended zone and the reduced zone. Because of the positions of As atoms, the translational lattice symmetry is reduced and the Brillouine zone is halved. In general, such a translational symmetry reduction may lead to hopping matrix between momentum $\mathbf{k}$ and $\mathbf{k}+\mathbf{Q}$ in the extended zone, with $\mathbf{Q} = (\pi,\pi)/a'$ and $a' = a/\sqrt{2}$ is the lattice constant of reduced unit cell. However, for the two orbitals d_{xz} and d_{yz}, the point-group symmetry prohibits the hybridization between states at $\mathbf{k}$ and $\mathbf{k}+\mathbf{Q}$ if we only consider intralayer hopping. The tight-binding Hamiltonian adopted by both Raghu *et al.*[27] and Lee and Wen[25] explicitly illustrate the vanishing of the mixing term. Therefore, we may discuss the SC symmetry using the extended zone and using H_0 given in Eq. (2). In the extended zone, there is only one Fermi point for each $\mathbf{k}$; hence the bands are not degenerate. In the weak pairing coupling limit, all the orbital antisymmetric pairing states will be irrelevant, and the weak-coupling theory will naturally lead to the orbital symmetric states.

Near the completion of the present work, we learned of the similar work by Wan and Wang[34] who considered SC symmetry for two-orbital pairing Hamiltonian. Our results are similar to theirs with the difference that we have included a spin-orbit coupling term in our group theory analysis, while this term was not explicitly included in Ref. 34. As a result, our classification for the spin triplet states is not the same as theirs. Such difference may be amplified when we discuss some behaviors related to spin degrees of freedom. We also note that similar group theory analysis were carried out for the two-band pairing Hamiltonian by Wang *et al.*[36] Since they adopted the bands instead of the orbitals, a direct comparison is not apparent. We become aware of another related work[37] after completing the present work too.

ACKNOWLEDGMENTS

We thank T. K. Ng and X. Dai for useful discussions and acknowledge HKSAR RGC grants for partial financial support.

APPENDIX A: SYMMETRY OF $\xi_{\mathbf{k}\alpha_1\alpha_2}$ IN EQUATION (2)

In this appendix, we will discuss the symmetry requirement of $\xi_{\mathbf{k}\alpha_1\alpha_2}$. The noninteracting Hamiltonian given by Eq. (2) should keep invariant under any symmetry transformation of point group D_4; hence H_0 belongs to the representation A_1. This symmetry requirement will affect the choice of $\xi_{\mathbf{k}\alpha_1\alpha_2}$. For convenience, we use the 2×2 matrix form $\hat{\xi}_{\mathbf{k}}$ in orbital space; thus $\hat{\xi}_{\mathbf{k}}$ can be rewritten in terms of Pauli matrices, $\hat{\xi}_{\mathbf{k}} = \xi^0_{\mathbf{k}}\sigma_0 + \xi^1_{\mathbf{k}}\sigma_1 + \xi^2_{\mathbf{k}}\sigma_2 + \xi^3_{\mathbf{k}}\sigma_3$. Similarly to the case of Ω, $\phi^\dagger_{\mathbf{k}s}\sigma_0\phi_{\mathbf{k}s}$, $\phi^\dagger_{\mathbf{k}s}\sigma_1\phi_{\mathbf{k}s}$, $\phi^\dagger_{\mathbf{k}s}\sigma_2\phi_{\mathbf{k}s}$, and $\phi^\dagger_{\mathbf{k}s}\sigma_3\phi_{\mathbf{k}s}$ transform as A_1, B_2, A_2, and B_1, respectively, where $\phi_{\mathbf{k}s} = (c_{\mathbf{k}1}, c_{\mathbf{k}2})^T$. Using the CG coefficients of $D_4 - C_4$ group chain,[32] we find that $\xi^0_{\mathbf{k}}$, $\xi^1_{\mathbf{k}}$, $\xi^2_{\mathbf{k}}$, and $\xi^3_{\mathbf{k}}$ transform as A_1, B_2, A_2, and B_1, respectively. Some examples of $\xi^{0,1,2,3}_{\mathbf{k}}$ are shown in the following:

$$\xi^0_{\mathbf{k}} = 1, \cos k_x + \cos k_y, \cos k_x \cos k_y,$$

$$\xi^1_{\mathbf{k}} = \sin k_x \sin k_y,$$

$$\xi^2_{\mathbf{k}} = \sin k_x \sin k_y (\cos k_x - \cos k_y),$$

$$\xi^3_{\mathbf{k}} = \cos k_x - \cos k_y.$$

APPENDIX B: POINT GROUP D_{4h}

Here we would like to specify the tetragonal point group according to the LaFeAsO space group $P4/nmm$.[31] In real space, the point group is neither usual $D_{4h} = D_4 \otimes \sigma_h$ nor usual D_4 generated by $\{C_{4z}, C_{2y}\}$, where σ_h is the reflection refer to xy plane, C_{4z} is the fourfold rotation around the z axis, and C_{2y} is the twofold rotation around the y axis, where (x,y,z) is specified in Fig. 2. However, it contains two subgroups, which refer to two different origin choices of the lattice. One is a subgroup of D_{4h} generated by $\{C_{4z}\sigma_h, C_{2y}\sigma_h\}$, which is also a D_4 group (or to be precise, D_{2d}, an isomorphic group to D_4) with origin choice 1 as shown in Figs. 1(a) and 2(a). The other subgroup is the direct product of inversion symmetry group I and cyclic group C_{2xy} with origin choice 2 as shown in Figs. 1(b) and 2(b). The transformation of (x,y,z) under these symmetry operations can be found in Tables V and VI. Hence in $\mathbf{k}$ space, it is still a tetragonal point group D_{4h}.

There are five irreducible representations of D_4 group; four of them, A_1, A_2, B_1, and B_2 are one-dimensional representations, and one of them E is a two-dimensional represen-

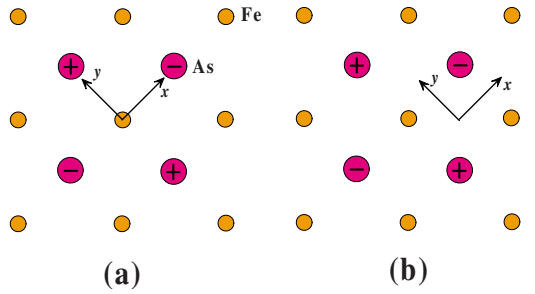

FIG. 2. (Color online) FeAs layer and specification of (x,y,z). xy plane consisting of Fe atoms is shown in (a) and (b) with different origin choices. The z axis is perpendicular to the Fe plane. "+" denotes an As atom above the Fe plane, while "–" denotes an As atom below the Fe plane. (a) Origin choice 1 and (b) origin choice 2 (also see Fig. 1).

tation. All these five representations are representations of group D_{4h} too. However, there are two two-dimensional irreducible representations E' and E'' of D_{4h} group, neither of them is the representation of group D_4. Naively, E' and E'' can be viewed as subrepresentations of two irreducible representations of group SU(2), $J=1/2$ and $J=3/2$, respectively. Since the representations E' and E'' cannot result in quadratic terms in Hamiltonian or Ginzburg-Landau free energy, we will not discuss them in this paper.

APPENDIX C: TRANSFORMATION OF GAP FUNCTIONS

It is not $\Delta(\mathbf{k})$ but $\psi(\mathbf{k})$ and $\mathbf{d}(\mathbf{k})$ transform as representations of symmetry group. In this appendix, we list the transformations of $\psi(\mathbf{k})$ and $\mathbf{d}(\mathbf{k})$ under various symmetry operations. First, under a point-group transformation g, $\psi(\mathbf{k})$ and $\mathbf{d}(\mathbf{k})$ transform as

$$g\psi(\mathbf{k}) = \psi(D^{-}_{(G)}(g)\mathbf{k}),$$

$$g\mathbf{d}(\mathbf{k}) = D^{+}_{(G)}(g)\mathbf{d}(D^{-}_{(G)}(g)\mathbf{k}), \tag{C1}$$

where $D^{\pm}_{(G)}(g)$ is the representation in three-dimensional space with positive (spin space) or negative ($\mathbf{k}$ space), respectively. Second, time-reversal transformations of $\psi(\mathbf{k})$ and $\mathbf{d}(\mathbf{k})$ take the forms

$$K\psi(\mathbf{k}) = \psi^*(-\mathbf{k}), \quad K\mathbf{d}(\mathbf{k}) = -\mathbf{d}^*(-\mathbf{k}). \tag{C2}$$

The antisymmetric nature of Fermion systems [see Eq. (5)] will lead to

$$\psi(-\mathbf{k}) = \psi(\mathbf{k}), \quad \mathbf{d}(-\mathbf{k}) = -\mathbf{d}(\mathbf{k}) \tag{C3}$$

for symmetric Ω and

$$\psi(-\mathbf{k}) = -\psi(\mathbf{k}), \quad \mathbf{d}(-\mathbf{k}) = \mathbf{d}(\mathbf{k}) \tag{C4}$$

for antisymmetric Ω. Hence, combining the above and the Hermitian choice of Ω's, the time-reversal invariance conditions for $\psi(\mathbf{k})$ and $\mathbf{d}(\mathbf{k})$ become

$$\psi^*(\mathbf{k}) = \psi(\mathbf{k}), \quad \mathbf{d}^*(\mathbf{k}) = \mathbf{d}(\mathbf{k}) \tag{C5}$$

since under time-reversal transformation, Ω transforms as

$$K\Omega = \Omega^*. \tag{C6}$$

TABLE V. Eight symmetry operations of D_{2d} (an isomorphic group to D_4) will generate eight general positions, where "general" is defined as the following: a set of symmetrical equivalent points is said to be in "general position" if each of its points is left invariant only by the identity operation but by no other symmetry operation of the space group. The origin choice is 1.

Group element	General position
E	(x,y,z)
$C_{4z}\sigma_h$	$(y,-x,-z)$
$(C_{4z}\sigma_h)^2$	$(-x,-y,z)$
$(C_{4z}\sigma_h)^3$	$(-y,x,-z)$
$C_{2y}\sigma_h$	$(-x,y,z)$
$C_{2y}\sigma_h C_{4z}\sigma_h$	$(-y,-x,-z)$
$C_{2y}\sigma_h(C_{4z}\sigma_h)^2$	$(x,-y,z)$
$C_{2y}\sigma_h(C_{4z}\sigma_h)^3$	$(y,x,-z)$

TABLE VI. Four symmetry operations and corresponding general positions of group $I\times C_{2xy}$. The origin choice is 2.

Group element	General position
E	(x,y,z)
C_i	$(-x,-y,-z)$
C_{2xy}	(y,x,z)
C_iC_{2xy}	$(-y,-x,-z)$

APPENDIX D: ENERGY GAP FUNCTIONS IN THE DEGENERATE BANDS

The energy gap of the superconducting states indeed depends on the details of interaction, especially, depends on the ratio of $\delta t/\lambda$, where δt is the energy scale of the splitting of two bands and λ is the energy scale of pairing potential. In the "strong pairing coupling" limit $\delta t \ll \lambda$, we expect the energy gap is close to $\delta t=0$ case; say, two bands are degenerate. A small perturbation proportional to $\delta t/\lambda$ will not change the energy gap very much, e.g., close the full gap or change from full gap to line nodal gap. In the weak pairing coupling limit $\lambda \ll \delta t$, the situation may be very different from strong-coupling limit, which is discussed in Ref. 34 so that we will focus on the strong-coupling limit and assume two degenerate bands in the following.

Due to two degenerate bands, the effective mean-field Hamiltonian in $\mathbf{k}$ space can be written as an 8×8 matrix,

$$\hat{H}_{\mathbf{k}} = \begin{pmatrix} \xi_{\mathbf{k}}\sigma_0 \otimes \sigma_0 & \Delta(\mathbf{k}) \\ \Delta^{\dagger}(\mathbf{k}) & -\xi_{\mathbf{k}}\sigma_0 \otimes \sigma_0 \end{pmatrix}, \tag{D1}$$

with the basis $\mathbf{c}_{\mathbf{k}} = (c_{\mathbf{k}\uparrow 1}, c_{\mathbf{k}\uparrow 2}, c_{\mathbf{k}\downarrow 1}, c_{\mathbf{k}\downarrow 2}, c^{\dagger}_{-\mathbf{k}\uparrow 1}, c^{\dagger}_{-\mathbf{k}\uparrow 2}, c^{\dagger}_{-\mathbf{k}\downarrow 1}, c^{\dagger}_{-\mathbf{k}\downarrow 2})^T$. The indices in the 4×4 matrices $\Delta(\mathbf{k})$ and $\xi_{\mathbf{k}}\sigma_0\otimes\sigma_0$ are arranged as follows: by direct products the former two indices denote spin space and the later two denote two orbitals. It is easy to know the energy dispersion,

$$E_{\mathbf{k}\mu} = \pm \sqrt{\xi_{\mathbf{k}}^2 + \Delta_{\mathbf{k}\mu}^2}, \tag{D2}$$

where $\Delta_{\mathbf{k}\mu}^2$ is one of the eigenvalues of the matrix $\Delta(\mathbf{k})\Delta^\dagger(\mathbf{k})$. For degenerate bands, the minimum of $|\Delta_{\mathbf{k}\mu}|$ is the energy gap. For simplicity, we will focus on the k_z-independent pairing with a cylinderlike Fermi surface which is the case of doped LaFeAsO most likely.

At first, we will consider the even-parity, orbital antisymmetric, and spin triplet pairing states in Table II. Orbital antisymmetric states have only one component σ_2 in the Ω part. Gap function is of the form $\Delta(\mathbf{k}) = i[\sigma \cdot \mathbf{d}(\mathbf{k})]\sigma_2 \otimes \sigma_2$, thus $\Delta_{\mathbf{k}\mu}^2 = |\mathbf{d}|^2 \pm |\mathbf{d} \times \mathbf{d}^*|$. For the time-reversal invariant state, $\mathbf{d} = \mathbf{d}^*$, the gapless condition follows as $|\mathbf{d}|^2 = 0$. For B_{1g} and B_{2g} states, they are d-wave states and have line nodal gap at Fermi surfaces. A_{1g} states can be of either s wave or extended s wave. The s-wave state is of full gap while the extended s-wave state possibly has line nodal gap at Fermi surface, e.g., the state $\mathbf{d}(\mathbf{k}) = \cos k_x \cos k_y \hat{z}$. The E_g representation involves s-wave, extended s-wave, and d-wave states. The s-wave state is fully gapful, the d-wave state has line nodal gap, and the extended s-wave state can be either fully gapful or of line nodal gap.

Then we consider the odd-parity, orbital symmetric, and spin triplet pairing states in Table IV. Orbital symmetric states have three components $\sigma_{0,1,3}$ in the Ω part. Gap function can be written as

$$\Delta(\mathbf{k}) = i[\sigma \cdot \mathbf{d}_0(\mathbf{k})]\sigma_2 \otimes \sigma_0 + i[\sigma \cdot \mathbf{d}_1(\mathbf{k})]\sigma_2 \otimes \sigma_1 + i[\sigma \cdot \mathbf{d}_3(\mathbf{k})]\sigma_2 \otimes \sigma_3, \tag{D3}$$

thus

$$\begin{aligned}\Delta(\mathbf{k})\Delta^\dagger(\mathbf{k}) = {} & [(|\mathbf{d}_0|^2 + |\mathbf{d}_1|^2 + |\mathbf{d}_3|^2)\sigma_0 + i(\mathbf{d}_0 \times \mathbf{d}_0^* + \mathbf{d}_1 \times \mathbf{d}_1^* + \mathbf{d}_3 \times \mathbf{d}_3^*) \cdot \sigma] \otimes \sigma_0 \\ & + [(\mathbf{d}_0 \cdot \mathbf{d}_1^* + \mathbf{d}_1 \cdot \mathbf{d}_0^*)\sigma_0 + i(\mathbf{d}_0 \times \mathbf{d}_1^* + \mathbf{d}_1 \times \mathbf{d}_0^*) \cdot \sigma] \otimes \sigma_1 + [(\mathbf{d}_0 \cdot \mathbf{d}_3^* + \mathbf{d}_3 \cdot \mathbf{d}_0^*)\sigma_0 + i(\mathbf{d}_0 \times \mathbf{d}_3^* + \mathbf{d}_3 \times \mathbf{d}_0^*) \cdot \sigma] \otimes \sigma_3 \\ & + [(\mathbf{d}_1 \times \mathbf{d}_3^* - \mathbf{d}_3 \times \mathbf{d}_1^*) \cdot \sigma - i(\mathbf{d}_1 \cdot \mathbf{d}_3^* - \mathbf{d}_3 \cdot \mathbf{d}_1^*)\sigma_0] \otimes \sigma_2. \end{aligned} \tag{D4}$$

For a time-reversal invariant state, $\mathbf{d}_i^*(\mathbf{k}) = \mathbf{d}_i(\mathbf{k})$, $i = 0, 1, 3$, so that the above can be simplified as

$$\Delta(\mathbf{k})\Delta^\dagger(\mathbf{k}) = (\mathbf{d}_0^2 + \mathbf{d}_1^2 + \mathbf{d}_3^2)\sigma_0 \otimes \sigma_0 + 2(\mathbf{d}_0 \cdot \mathbf{d}_1)\sigma_0 \otimes \sigma_1 + 2(\mathbf{d}_0 \cdot \mathbf{d}_3)\sigma_0 \otimes \sigma_3 + 2(\mathbf{d}_1 \times \mathbf{d}_3) \cdot \sigma \otimes \sigma_2. \tag{D5}$$

We obtain from the above

$$\Delta_{\mathbf{k}\mu}^2 = (\mathbf{d}_0^2 + \mathbf{d}_1^2 + \mathbf{d}_3^2) \pm 2\sqrt{(\mathbf{d}_0 \cdot \mathbf{d}_1)^2 + (\mathbf{d}_0 \cdot \mathbf{d}_3)^2 + (\mathbf{d}_1 \times \mathbf{d}_3)^2}. \tag{D6}$$

Gapless condition reads

$$\mathbf{d}_0^2 + \mathbf{d}_1^2 + \mathbf{d}_3^2 = 2\sqrt{(\mathbf{d}_0 \cdot \mathbf{d}_1)^2 + (\mathbf{d}_0 \cdot \mathbf{d}_3)^2 + (\mathbf{d}_1 \times \mathbf{d}_3)^2}. \tag{D7}$$

Careful analysis shows that node can appear only when at least one of $|\mathbf{d}_0|$, $|\mathbf{d}_1|$, and $|\mathbf{d}_3|$ vanishes so that E_u states in Table IV are of line nodal gap. The other four representations A_{1u}, A_{2u}, B_{1u}, and B_{2u} can be of either line nodal or full gap. For example, for an A_{1u} states in Table IV which consists of two components in the Ω part, $\mathbf{d}_0(\mathbf{k}) = \sin k_x \hat{x} + \sin k_y \hat{y}$, $\mathbf{d}_3(\mathbf{k}) = \sin k_x \hat{x} - \sin k_y \hat{y}$, and $\mathbf{d}_1(\mathbf{k}) = 0$, nodal lines will appear at $\sin k_x = 0$ and $\sin k_y = 0$. Moreover, any A_{1u} state in Table IV which consists of only one component in the Ω part is of full gap.

Similar consideration will lead to the results for spin singlet states shown in Tables I and III. Of course, when the ratio $\delta t/\lambda$ becomes large, the situation may change. This change strongly depends on the details of both pairing states and the Hamiltonian. For example, for an s wave with $\mathbf{d}(\mathbf{k}) = \hat{z}$ and $\Omega = \sigma_2$, Fermi pockets may appear when δt and λ are comparable.

[1] M. Sigrist and K. Ueda, Rev. Mod. Phys. **63**, 239 (1991).

[2] Y. Kamihara, T. Watanabe, M. Hirano, and H. Hosono, J. Am. Chem. Soc. **130**, 3296 (2008); H. Takahashi, K. Igawa, K. Arii, Y. Kamihara, M. Hirano, and H. Hosono, Nature (London) **453**, 376 (2008).

[3] G. F. Chen, Z. Li, D. Wu, G. Li, W. Z. Hu, J. Dong, P. Zheng, J. L. Luo, and N. L. Wang, Phys. Rev. Lett. **100**, 247002 (2008).

[4] X. H. Chen, T. Wu, G. Wu, R. H. Liu, H. Chen, and D. F. Fang, Nature (London) **453**, 761 (2008).

[5] Z. A. Ren, J. Yang, W. Lu, W. Yi, G. C. Che, X. L. Dong, L. L. Sun, and Z. X. Zhao, Mater. Res. Innovations **12**, 1 (2008).

[6] Z. A. Ren, W. Lu, J. Yang, W. Yi, X. L. Shen, Z. C. Li, G. C. Che, X. L. Dong, L. L. Sun, F. Zhou, and Z. X. Zhao, Chin. Phys. Lett. **25**, 2215 (2008).

[7] C. Wang, L. J. Li, S. Chi, Z. W. Zhu, Z. Ren, Y. K. Li, Y. T. Wang, X. Lin, Y. K. Luo, X. F. Xu, G. H. Cao, and Z. A. Xu, arXiv:0804.4290 (unpublished).

[8] Z. A. Ren, G. C. Che, X. L. Dong, J. Yang, W. Lu, W. Yi, X. L. Shen, Z. C. Li, L. L. Sun, F. Zhou, and Z. X. Zhao, Europhys. Lett. **83**, 17002 (2008).

[9] H. H. Wen, G. Mu, L. Fang, H. Yang, and X. Y. Zhu, Europhys. Lett. **82**, 17009 (2008).

[10] J. Dong, H. J. Zhang, G. Xu, Z. Li, G. Li, W. Z. Hu, D. Wu, G. F. Chen, X. Dai, J. L. Luo, Z. Fang, and N. L. Wang, Europhys. Lett. **83**, 27006 (2008).

[11] Clarina de la Cruz, Q. Huang, J. W. Lynn, J. Y. Li, W. Ratcliff II,

J. L. Zarestky, H. A. Mook, G. F. Chen, J. L. Luo, N. L. Wang and P. C. Dai, Nature (London) **453**, 899 (2008).
[12] M. Gang, X. Zhu, L. Fang, L. Shan, C. Ren, and H. H. Wen, Chin. Phys. Lett. **25**, 2221 (2008).
[13] K. Ahilan, F. L. Ning, T. Imai, A. S. Sefat, R. Jin, M. A. McGuire, B. C. Sales, and D. Mandrus, arXiv:0804.4026 (unpublished).
[14] Y. Nakai, K. Ishida, Y. Kamihara, M. Hirano, and H. Hosono, J. Phys. Soc. Jpn. **77**, 073701 (2008).
[15] K. Matano, Z. A. Ren, X. L. Dong, L. L. Sun, Z. X. Zhao, and G. Q. Zheng, Europhys. Lett. **83**, 57001 (2008).
[16] L. Boeri, O. V. Dolgov, and A. A. Golubov, Phys. Rev. Lett. **101**, 026403 (2008).
[17] D. J. Singh and M. H. Du, Phys. Rev. Lett. **100**, 237003 (2008).
[18] K. Haule, J. H. Shim, and G. Kotliar, Phys. Rev. Lett. **100**, 226402 (2008).
[19] G. Xu, W. Ming, Y. Yao, X. Dai, S. C. Zhang, and Z. Fang, Europhys. Lett. **82**, 67002 (2008).
[20] I. I. Mazin, D. J. Singh, M. D. Johannes, and M. H. Du, Phys. Rev. Lett. **101**, 057003 (2008).
[21] C. Cao, P. J. Hirschfeld, and H. P. Cheng, Phys. Rev. B **77**, 220506(R) (2008).
[22] F. J. Ma and Z. Y. Lu, Phys. Rev. B **78**, 033111 (2008).
[23] X. Dai, Z. Fang, Y. Zhou, and F. C. Zhang, Phys. Rev. Lett. **101**, 057008 (2008).
[24] T. Li, arXiv:0804.0536 (unpublished).
[25] P. A. Lee and X. G. Wen, arXiv:0804.1739 (unpublished).
[26] Z. Y. Weng, arXiv:0804.3228 (unpublished).
[27] S. Raghu, X. L. Qi, C. X. Liu, D. J. Scalapino, and S. C. Zhang, Phys. Rev. B **77**, 220503(R) (2008).
[28] Z. J. Yao, J. X. Li, and Z. D. Wang, arXiv:0804.4166 (unpublished).
[29] Q. M. Si and E. Abrahams, arXiv:0804.2480, Phys. Rev. Lett.(to be published).
[30] T. A. Maier and D. J. Scalapino, arXiv:0805.0316 (unpublished).
[31] *International Tables for Crystallography*, Space-Group Symmetry Vol. I, 4th ed. (Kluwer, Dordrecht, The Nertherlands, 1996).
[32] P. H. Butler, *Point Group Symmetry Applications: Methods and Tables* (Plenum, New York, 1981).
[33] If the lattice undergoes a structural transition, e.g., the transition from tetragonal ($P4/nmm$) to monoclinic ($P112/n$) in the parent compound LaFeAsO, lattice symmetry will be reduced and thereby the pairing states within each representation of D_4 will be further splitted by energy. However, P_{space}, P_{spin}, and P_{orbital} considered in this paper are still good quantum numbers. Moreover, when the monoclinic distortion to tetragonal phase is small as in practice (Ref. 11), our study is a good approximation to such a monoclinic lattice.
[34] Y. Wan and Q. H. Wang, arXiv:0805.0923 (unpublished).
[35] M. Daghofer, A. Moreo, J. A. Riera, E. Arrigoni, and E. Dagotto, arXiv:0805.0148 (unpublished).
[36] Z. H. Wang, H. Tang, Z. Fang, and X. Dai, arXiv:0805.0736 (unpublished).
[37] J. R. Shi, arXiv:0806.0259 (unpublished).